Maejo Int. J. Sci. Technol. **2015**, *9*(02), 224-245

Maejo International Journal of Science and Technology

ISSN 1905-7873
Available online at www.mijst.mju.ac.th

Full Paper

Soret effects on unsteady magnetohydrodynamic mixed-convection heat-and-mass-transfer flow in a porous medium with Newtonian heating

Abid Hussanan [1], Mohd Z. Salleh [1,*], Ilyas Khan [2], Razman M. Tahar [3] and Zulkhibri Ismail [1]

[1] Applied and Industrial Mathematics Research Group, Faculty of Industrial Science and Technology, Universiti Malaysia Pahang, Lebuhraya Tun Razak, 26300 UMP Kuantan, Pahang, Malaysia
[2] College of Engineering, Majmaah University, P.O. Box 66, Majmaah 11952, Saudi Arabia
[3] Faculty of Industrial Management, Universiti Malaysia Pahang, Lebuhraya Tun Razak, 26300 UMP Kuantan, Pahang, Malaysia
* Corresponding author, e-mail: zukikuj@yahoo.com

Received: 31 May 2014 / Accepted: 4 August 2015 / Published: 5 August 2015

Abstract: Soret effects on unsteady mixed-convection heat-and-mass-transfer flow over an oscillating vertical plate embedded in a porous medium with Newtonian heating in the presence of magnetic field are studied. The governing equations, along with imposed initial and boundary conditions, are first converted into the dimensionless form and then solved using the Laplace transform technique. The numerical results for fluid velocity, temperature and concentration are graphically shown, whereas the skin friction, Nusselt number and Sherwood number are presented in tabular forms. It is observed that the fluid velocity and concentration increase with increasing values of Soret number. The conjugate parameter of Newtonian heating increases the temperature as well as the concentration and velocity distributions. It is also found that the rates of the heat-and-mass transfer increase as the conjugate parameter increases.

Keywords: Soret effects, magnetohydrodynamic flow, heat-and-mass-transfer flow, porous medium, Newtonian heating

INTRODUCTION

Recently the study of magnetohydrodynamic (MHD) flow, together with heat-and-mass transfer, has received the attention of a large number of researchers because of its diverse applications in many branches of science and technology as well in industry. Some of the important applications are found in stellar and solar structures, cooling of nuclear reactors, interstellar matter,

Maejo Int. J. Sci. Technol. **2015**, *9*(02), 224-245

liquid metal fluid, power generation system, radio propagation, aero dynamics and electromagnetic material processing [1-3]. Suneetha et al. [4], for instance, studied the MHD heat-and-mass transfer flow past a vertical plate with variable surface temperature by considering the heat due to viscous dissipation. The effects of thermal radiation and chemical reaction on MHD free-convection flow past a semi-infinite inclined porous plate with variable surface temperature and concentration were studied by Uddin and Kumar [5]. The same problem was considered by Muthucumaraswamy and Valliammal [6] for an exponentially accelerated infinite vertical plate without thermal radiation effect. Recently, Nandkeolyar et al. [7] obtained an exact solution of unsteady MHD free-convection heat-and-mass-transfer flow in a heat absorbing fluid with ramped wall temperature.

On the other hand, the problem of MHD mixed-convection flow through porous media has been the subject of considerable research activity in recent years because of its several important applications such as those involving heat removal from nuclear fuel debris, drug permeation through human skin, oil flow through porous rock and filtration of solids from liquids [8, 9]. Beg et al. [10] presented exact solutions for unsteady MHD heat transfer in a semi-infinite porous medium with thermal radiation flux. In the same year, Reddy et al. [11] extended the work of Beg et al. [10] by taking into account the periodic wall temperature. The effects of thermal radiation on MHD free-convection flow through a porous medium with variable boundary conditions were investigated by Kishore et al. [12]. The effects of slip condition on the unsteady MHD flow of a viscoelastic fluid in a porous channel were analysed by Farhad et al. [13]. Recently, the influence of thermal radiation and chemical reaction on MHD heat-and-mass-transfer flow embedded in a porous medium with variable suction was studied by Ahmed and Das [14].

In all the above studies, the thermal-diffusion (Soret) effect was neglected. Thermal diffusion of great significance for isotope separation and for making a mixture of gases with very light molecular weights (H_2, He) and medium molecular weights (N_2, air) [15]. Due to the importance of thermal-diffusion effect, a number of researchers have studied it for different fluids. Ahmed [16], for instance, made an exact analysis of the thermal-diffusion effect on combined heat-and-mass-transfer Hartmann flow through a channel bounded by two infinite horizontal isothermal parallel plates. The Soret-driven, free-convection heat-and-mass-transfer flow of a non-Newtonian liquid past a vertical plate in a thermally stratified porous medium was studied by Narayana et al. [17]. Farhad et al. [18] found analytical solutions of MHD heat-and-mass-transfer flow past a vertical plate embedded in a porous medium in the presence of Soret and chemical effects. The influence of Soret effect on the unsteady motion of MHD mixed-convection flow of a viscoelastic fluid over an infinite vertical plate in the presence of a heat source was investigated by Jha et al. [19]. Sharma et al. [20] studied the Soret and Dufour effects on unsteady MHD mixed-convection flow with heat source and Ohmic dissipation. Recently, MHD heat-and-mass-transfer flow over a vertical plate in a porous medium under the influence of Dufour and Soret effects was discussed by Vedavathi et al. [21].

The mixed convection flows with combined heat-and-mass transfer past an oscillating vertical plate are usually modelled by considering the ramped wall temperature, variable surface temperature or constant surface heat-flux boundary conditions [22-24]. However, in many practical situations where the heat transfer from the surface is proportional to the local surface temperature, the above conditions fail to work and the Newtonian heating condition is needed. Merkin [25] initiated the idea of Newtonian heating in his pioneering work on natural convection boundary flow passing through a vertical surface. Applications of Newtonian heating are found in many important engineering applications, e.g. in heat exchangers where bounding surfaces absorb heat by solar

Maejo Int. J. Sci. Technol. **2015**, *9*(02), 224-245

radiation and in conjugate heat transfer around fins. Considering the importance of Newtonian heating condition, many authors have used it in their convective heat-transfer problems and obtained the solutions either numerically [26-30] or analytically [31-38]. The main objective of the present study is to investigate the thermal-diffusion effect on unsteady MHD mixed-convection heat-and-mass-transfer flow past an oscillating vertical plate through a porous medium with Newtonian heating, where the heat transfer from the surface is proportional to the local surface temperature. The governing equations are solved using Laplace transform technique and the expressions for velocity, temperature and concentration are obtained in terms of exponential and complementary error functions. The corresponding expressions for skin friction, Nusselt number and Sherwood number are also evaluated.

MATHEMATICAL FORMULATION

Consider the unsteady mixed convection flow of a viscous incompressible fluid through a porous medium bounded by an infinite oscillating vertical plate. The x'-axis is taken along the vertical plate and y'-axis normal to it. The magnetic field B_0 of uniform strength is applied normal to the plate and the induced magnetic field is considered to be negligible. Initially, for time $t' \le 0$, both the plate and fluid are at rest with constant temperature T_∞ and concentration C_∞. At time $t' = 0^+$, the plate starts an oscillatory motion in its plane with velocity $\boldsymbol{V}$:

$$\boldsymbol{V} = U_0 \cos(\omega' t')\mathbf{i};\ t' > 0, \tag{1}$$

where $\mathbf{i}$ is the unit vector in the flow direction, U_0 is the amplitude of the plate oscillations and ω' is the frequency of oscillation. At the same time, the heat transfer from the plate to the fluid is proportional to the local surface temperature T' and the concentration near the plate is raised from C_∞ to C_w. The geometry of the problem is shown in Figure 1.

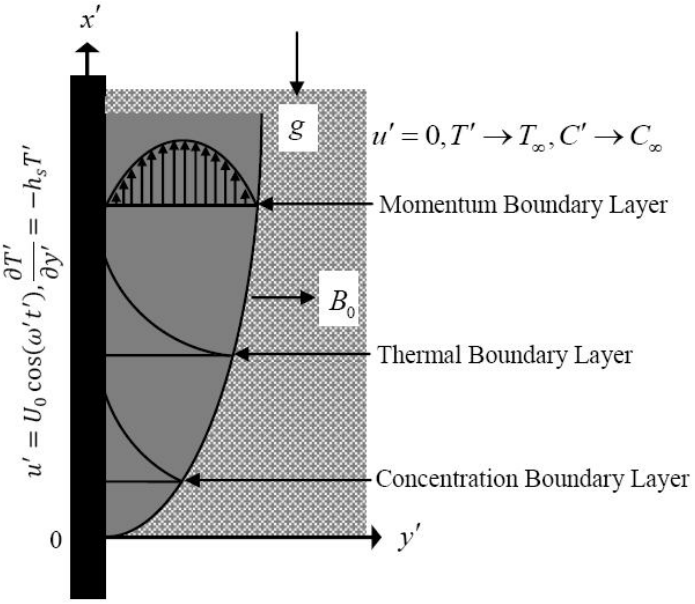

Figure 1. Physical sketch of different boundary layers in a porous medium under the effect of magnetic field, together with the corresponding Cartesian coordinates

Maejo Int. J. Sci. Technol. **2015**, *9*(02), 224-245

Under the Boussinesq's approximation [39], the governing equations of free convection flow can be written as:

$$\frac{\partial u'}{\partial t'} = \nu \frac{\partial^2 u'}{\partial y'^2} - \frac{\sigma B_0^2}{\rho} u' - \frac{\nu \phi}{k_1} u' + g\beta\left(T' - T_\infty\right) + g\beta^*\left(C' - C_\infty\right), \tag{2}$$

$$\rho C_p \frac{\partial T'}{\partial t'} = k \frac{\partial^2 T'}{\partial y'^2} - \frac{\partial q_r}{\partial y'}, \tag{3}$$

$$\frac{\partial C'}{\partial t'} = D \frac{\partial^2 C'}{\partial y'^2} + \frac{DK_T}{T_m} \frac{\partial^2 T'}{\partial y'^2}, \tag{4}$$

where u' is the axial velocity, t' the time, ρ the fluid density, ν the kinematic viscosity, σ the electric conductivity of the fluid, ϕ the porosity, k_1 the permeability, g the acceleration due to gravity, β the volumetric coefficient of thermal expansion, β^* the volumetric coefficient of mass expansion, C_p the heat capacity at constant pressure, T' the temperature of the fluid, k the thermal conductivity, q_r the radiative flux along the y'-axis, C' the species concentration in the fluid, C_∞ the species concentration far away from the plate, K_T the thermal diffusion ratio, T_∞ the ambient temperature, T_m the mean fluid temperature and D the mass diffusivity.

The corresponding initial and boundary conditions are

$$t' \le 0 \ : \ u' = 0, \ T' = T_\infty, \ C' = C_\infty \text{ for all } y' \ge 0, \tag{5}$$

$$t' > 0 \ : \ u' = U_0 \cos\left(\omega' t'\right), \ \frac{\partial T'}{\partial y'} = -h_s T', \ C' = C_w \text{ at } y' = 0, \tag{6}$$

$$u' \to 0, \ T' \to T_\infty, \ C' \to C_\infty \text{ as } y' \to \infty, \tag{7}$$

where h_s is the heat transfer coefficient, and C_∞ and C_w are the species concentrations near and far away from the plate respectively. Using the Rosseland approximation [40], equation (3) modifies to:

$$\rho C_p \frac{\partial T'}{\partial t'} = k\left(1 + \frac{16\sigma^* T_\infty^3}{3kk^*}\right)\frac{\partial^2 T'}{\partial y'^2}. \tag{8}$$

Introducing the following non-dimensional variables,

$$y = \frac{y' U_0}{\nu}, \ t = \frac{t' U_0^2}{\nu}, \ u = \frac{u'}{U_0}, \ \theta = \frac{T' - T_\infty}{T_\infty}, \ C = \frac{C' - C_\infty}{C_w - C_\infty}, \ \omega = \frac{\omega' \nu}{U_0^2},$$

into equations (2), (4) and (8), we obtain

$$\frac{\partial u}{\partial t} = \frac{\partial^2 u}{\partial y^2} - M^2 u - \frac{1}{K} u + Gr\theta + GmC, \tag{9}$$

$$\Pr \frac{\partial \theta}{\partial t} = \left(1 + R\right)\frac{\partial^2 \theta}{\partial y^2}, \tag{10}$$

$$\frac{\partial C}{\partial t} = \frac{1}{Sc}\frac{\partial^2 C}{\partial y^2} + Sr \frac{\partial^2 \theta}{\partial y^2}, \tag{11}$$

Maejo Int. J. Sci. Technol. **2015**, *9*(02), 224-245

where

$$Gr=\frac{\nu g\beta T_\infty}{U_0^3},\ Gm=\frac{\nu g\beta^*\left(C_w-C_\infty\right)}{U_0^3},\ M^2=\frac{\nu\sigma B_0^2}{\rho U_0^2},\ \frac{1}{K}=\frac{\nu^2\phi}{k_1U_0^2},$$

$$\Pr=\frac{\mu C_p}{k},\ R=\frac{16\sigma^*T_\infty^3}{3kk^*},\ Sc=\frac{\nu}{D},\ Sr=\frac{DK_TT_\infty}{\nu T_m\left(C_w-C_\infty\right)},$$

are the Grashof number, modified Grashof number, magnetic parameter, porosity parameter, Prandtl number, radiation parameter, Schmidt number and Soret number respectively. The corresponding initial and boundary conditions in non-dimensional forms are:

$$t\le 0\ :\ u=0,\ \theta=0,\ C=0\ \text{ for all } y\ge 0, \tag{12}$$

$$t>0\ :\ u=\cos\left(\omega t\right),\ \frac{\partial\theta}{\partial y}=-\gamma\left(1+\theta\right),\ C=1\ \text{ at } y=0, \tag{13}$$

$$u\to 0,\ \theta\to 0,\ C\to 0\ \text{ as } y\to\infty. \tag{14}$$

Here, $\gamma=h_s\nu/U_0$ is the conjugate parameter for Newtonian heating. It is important to note that equation (13) gives $\theta=0$ when $\gamma=0$, corresponding to $h_s=0$ and consequently, in this case no heating from the plate exists [27, 33].

METHOD OF SOLUTIONS

Applying the Laplace transform with respect to time t to the system of equations (9) to (14), we obtain the following solutions in the transformed (y,q) plane:

$$\begin{aligned}\bar{u}(y,q)=&\frac{1}{2\left(q+i\omega\right)}e^{-y\sqrt{q+L}}+\frac{1}{2\left(q-i\omega\right)}e^{-y\sqrt{q+L}}+\frac{ac}{q^2\left(\sqrt{q}-c\right)}e^{-y\sqrt{q+L}}\\&-\frac{cdh}{q^2\left(\sqrt{q}-c\right)}e^{-y\sqrt{q+L}}+\frac{bch}{q^2\left(\sqrt{q}-c\right)}e^{-y\sqrt{q+L}}+\frac{b}{q^2}e^{-y\sqrt{q+L}}\\&-\frac{ac}{q^2\left(\sqrt{q}-c\right)}e^{-y\sqrt{q\,\Pr_{\text{eff}}}}+\frac{cdh}{q^2\left(\sqrt{q}-c\right)}e^{-y\sqrt{q\,\Pr_{\text{eff}}}}-\frac{b}{q^2}e^{-y\sqrt{qSc}}\\&-\frac{bch}{q^2\left(\sqrt{q}-c\right)}e^{-y\sqrt{qSc}},\end{aligned} \tag{15}$$

$$\bar{\theta}\left(y,q\right)=\frac{c}{q\left(\sqrt{q}-c\right)}e^{-y\sqrt{q\,\Pr_{\text{eff}}}}, \tag{16}$$

$$\bar{C}(y,q)=\frac{1}{q}e^{-y\sqrt{qSc}}+\frac{ch}{q\left(\sqrt{q}-c\right)}e^{-y\sqrt{qSc}}-\frac{ch}{q\left(\sqrt{q}-c\right)}e^{-y\sqrt{q\,\Pr_{\text{eff}}}}, \tag{17}$$

where $\bar{u}\left(y,q\right)=\int_0^\infty e^{-qt}u\left(y,t\right)dt$, $\bar{\theta}\left(y,q\right)=\int_0^\infty e^{-qt}\theta\left(y,t\right)dt$ and $\bar{C}\left(y,q\right)=\int_0^\infty e^{-qt}C\left(y,t\right)dt$ denote the Laplace transforms of $u\left(y,t\right)$, $\theta\left(y,t\right)$ and $C\left(y,t\right)$ respectively, and $a=\frac{Gr}{\Pr_{\text{eff}}-1}$, $b=\frac{Gm}{Sc-1}$, $c=\frac{\gamma}{\sqrt{\Pr_{\text{eff}}}}$, $d=\frac{Gm}{\Pr_{\text{eff}}-1}$, $h=\frac{ScSr\,\Pr_{\text{eff}}}{\Pr_{\text{eff}}-1}$, $L=M^2+\frac{1}{K}$ and $\Pr_{\text{eff}}=\frac{\Pr}{1+R}$ ($\Pr_{\text{eff}}$ = the effective Prandtl number) [40]. The inverse Laplace transform of equations (15) to (17) yields:

Maejo Int. J. Sci. Technol. **2015**, *9*(02), 224-245

$$\theta(y,t)=e^{\left(c^2t-yc\sqrt{\mathrm{Pr}_{\mathrm{eff}}}\right)}\mathrm{erfc}\left(\frac{y}{2}\sqrt{\frac{\mathrm{Pr}_{\mathrm{eff}}}{t}}-c\sqrt{t}\right)-\mathrm{erfc}\left(\frac{y}{2}\sqrt{\frac{\mathrm{Pr}_{\mathrm{eff}}}{t}}\right), \tag{18}$$

$$\begin{aligned}C(y,t)=&\,\mathrm{erfc}\left(\frac{y}{2}\sqrt{\frac{Sc}{t}}\right)+h\left[e^{\left(c^2t-yc\sqrt{Sc}\right)}\mathrm{erfc}\left(\frac{y}{2}\sqrt{\frac{Sc}{t}}-c\sqrt{t}\right)-\mathrm{erfc}\left(\frac{y}{2}\sqrt{\frac{Sc}{t}}\right)\right]\\&-h\left[e^{\left(c^2t-yc\sqrt{\mathrm{Pr}_{\mathrm{eff}}}\right)}\mathrm{erfc}\left(\frac{y}{2}\sqrt{\frac{\mathrm{Pr}_{\mathrm{eff}}}{t}}-c\sqrt{t}\right)-\mathrm{erfc}\left(\frac{y}{2}\sqrt{\frac{\mathrm{Pr}_{\mathrm{eff}}}{t}}\right)\right],\end{aligned} \tag{19}$$

$$\begin{aligned}u(y,t)=&\frac{1}{4}e^{-i\omega t}\left[e^{-y\sqrt{L-i\omega}}\mathrm{erfc}\left(\frac{y}{2\sqrt{t}}-\sqrt{(L-i\omega)t}\right)+e^{y\sqrt{L-i\omega}}\mathrm{erfc}\left(\frac{y}{2\sqrt{t}}+\sqrt{(L-i\omega)t}\right)\right]\\&+\frac{1}{4}e^{i\omega t}\left[e^{-y\sqrt{L+i\omega}}\mathrm{erfc}\left(\frac{y}{2\sqrt{t}}-\sqrt{(L+i\omega)t}\right)+e^{y\sqrt{L+i\omega}}\mathrm{erfc}\left(\frac{y}{2\sqrt{t}}+\sqrt{(L+i\omega)t}\right)\right]\\&+\frac{(dh-a)}{c^2}\left[e^{\left(c^2t-yc\sqrt{\mathrm{Pr}_{\mathrm{eff}}}\right)}\mathrm{erfc}\left(\frac{y}{2}\sqrt{\frac{\mathrm{Pr}_{\mathrm{eff}}}{t}}-c\sqrt{t}\right)-\mathrm{erfc}\left(\frac{y}{2}\sqrt{\frac{\mathrm{Pr}_{\mathrm{eff}}}{t}}\right)\right]\\&-\frac{(dh-a)}{c}\left[2\sqrt{\frac{t}{\pi}}e^{-\frac{y^2\mathrm{Pr}_{\mathrm{eff}}}{4t}}-y\sqrt{\mathrm{Pr}_{\mathrm{eff}}}\,\mathrm{erfc}\left(\frac{y}{2}\sqrt{\frac{\mathrm{Pr}_{\mathrm{eff}}}{t}})\right)\right]\\&-(dh-a)\left[\left(\frac{y^2\mathrm{Pr}_{\mathrm{eff}}}{2}+t\right)\mathrm{erfc}\left(\frac{y}{2}\sqrt{\frac{\mathrm{Pr}_{\mathrm{eff}}}{t}}\right)-y\sqrt{\mathrm{Pr}_{\mathrm{eff}}}\sqrt{\frac{t}{\pi}}e^{-\frac{y^2\mathrm{Pr}_{\mathrm{eff}}}{4t}}\right]\\&-\frac{bh}{c^2}\left[e^{\left(c^2t-yc\sqrt{Sc}\right)}\mathrm{erfc}\left(\frac{y}{2}\sqrt{\frac{Sc}{t}}-c\sqrt{t}\right)-\mathrm{erfc}\left(\frac{y}{2}\sqrt{\frac{Sc}{t}}\right)\right]\\&+\frac{bh}{c}\left[2\sqrt{\frac{t}{\pi}}e^{-\frac{y^2Sc}{4t}}-y\sqrt{Sc}\,\mathrm{erfc}\left(\frac{y}{2}\sqrt{\frac{Sc}{t}}\right)\right]\\&+b(h-1)\left[\left(\frac{y^2Sc}{2}+t\right)\mathrm{erfc}\left(\frac{y}{2}\sqrt{\frac{Sc}{t}}\right)-y\sqrt{Sc}\sqrt{\frac{t}{\pi}}e^{-\frac{y^2Sc}{4t}}\right]\\&+\frac{bt}{2}\left[e^{-y\sqrt{L}}\mathrm{erfc}\left(\frac{y}{2\sqrt{t}}-\sqrt{Lt}\right)+e^{y\sqrt{L}}\mathrm{erfc}\left(\frac{y}{2\sqrt{t}}+\sqrt{Lt}\right)\right]\\&-\frac{yb}{4\sqrt{L}}\left[e^{-y\sqrt{L}}\mathrm{erfc}\left(\frac{y}{2\sqrt{t}}-\sqrt{Lt}\right)-e^{y\sqrt{L}}\mathrm{erfc}\left(\frac{y}{2\sqrt{t}}+\sqrt{Lt}\right)\right]\\&+c(a-dh+bh)\int_0^t\left[\frac{1}{\sqrt{\pi(t-s)}}+ce^{c^2(t-s)}\mathrm{erfc}\left(-c\sqrt{t-s}\right)\right]\\&\times\left[\left(\tfrac{s}{2}-\tfrac{y}{4\sqrt{L}}\right)e^{-y\sqrt{L}}\mathrm{erfc}\left(\tfrac{y}{2\sqrt{s}}-\sqrt{Ls}\right)+\left(\tfrac{s}{2}+\tfrac{y}{4\sqrt{L}}\right)e^{y\sqrt{L}}\mathrm{erfc}\left(\tfrac{y}{2\sqrt{s}}+\sqrt{Ls}\right)\right]ds.\end{aligned} \tag{20}$$

where $\mathrm{erfc}(.)$ represents the complementary error function.

Note that the above solutions for concentration and velocity given by equations (19) and (20) are only valid for $\mathrm{Pr}_{\mathrm{eff}}\neq 1$ and $Sc\neq 1$. Moreover, the other solutions are:

Maejo Int. J. Sci. Technol. **2015**, *9*(02), 224-245

1) When $\mathrm{Pr}_{\mathrm{eff}}=1$ and $Sc\neq 1$,

$$C(y,t)=\operatorname{erfc}\left(\frac{y}{2}\sqrt{\frac{Sc}{t}}\right)-\frac{ScSr}{(Sc-1)}\left[e^{\left(\gamma^2 t-y\gamma\sqrt{Sc}\right)}\operatorname{erfc}\left(\frac{y}{2}\sqrt{\frac{Sc}{t}}-\gamma\sqrt{t}\right)-\operatorname{erfc}\left(\frac{y}{2}\sqrt{\frac{Sc}{t}}\right)\right]$$
$$+\frac{ScSr}{(Sc-1)}\left[e^{\left(\gamma^2 t-y\gamma\right)}\operatorname{erfc}\left(\frac{y}{2\sqrt{t}}-c\sqrt{t}\right)-\operatorname{erfc}\left(\frac{y}{2\sqrt{t}}\right)\right], \tag{21}$$

$$u(y,t)=\frac{1}{4}e^{-i\omega t}\left[e^{-y\sqrt{L-i\omega}}\operatorname{erfc}\left(\frac{y}{2\sqrt{t}}-\sqrt{(L-i\omega)t}\right)+e^{y\sqrt{L-i\omega}}\operatorname{erfc}\left(\frac{y}{2\sqrt{t}}+\sqrt{(L-i\omega)t}\right)\right]$$
$$+\frac{1}{4}e^{i\omega t}\left[e^{-y\sqrt{L+i\omega}}\operatorname{erfc}\left(\frac{y}{2\sqrt{t}}-\sqrt{(L+i\omega)t}\right)+e^{y\sqrt{L+i\omega}}\operatorname{erfc}\left(\frac{y}{2\sqrt{t}}+\sqrt{(L+i\omega)t}\right)\right]$$
$$+\left(\frac{Gr+bScSr}{L}\right)\left[e^{\left(\gamma^2 t-y\gamma\right)}\operatorname{erfc}\left(\frac{y}{2\sqrt{t}}-\gamma\sqrt{t}\right)-\operatorname{erfc}\left(\frac{y}{2\sqrt{t}}\right)\right]$$
$$+\frac{bScSr}{\gamma^2\left(Sc-1\right)}\left[e^{\left(\gamma^2 t-y\gamma\sqrt{Sc}\right)}\operatorname{erfc}\left(\frac{y}{2}\sqrt{\frac{Sc}{t}}-\gamma\sqrt{t}\right)-\operatorname{erfc}\left(\frac{y}{2}\sqrt{\frac{Sc}{t}}\right)\right]$$
$$-\frac{bScSr}{\gamma\left(Sc-1\right)}\left[2\sqrt{\frac{t}{\pi}}e^{-\frac{y^2Sc}{4t}}-y\sqrt{Sc}\operatorname{erfc}\left(\frac{y}{2}\sqrt{\frac{Sc}{t}}\right)\right]$$
$$-\frac{bScSr}{\left(Sc-1\right)}\left[\left(\frac{y^2Sc}{2}+t\right)\operatorname{erfc}\left(\frac{y}{2}\sqrt{\frac{Sc}{t}}\right)-y\sqrt{Sc}\sqrt{\frac{t}{\pi}}e^{-\frac{y^2Sc}{4t}}\right]$$
$$-b\left[\left(\frac{y^2Sc}{2}+t\right)\operatorname{erfc}\left(\frac{y}{2}\sqrt{\frac{Sc}{t}}\right)-y\sqrt{Sc}\sqrt{\frac{t}{\pi}}e^{-\frac{y^2Sc}{4t}}\right]$$
$$+\frac{bt}{2}\left[e^{-y\sqrt{L}}\operatorname{erfc}\left(\frac{y}{2\sqrt{t}}-\sqrt{Lt}\right)+e^{y\sqrt{L}}\operatorname{erfc}\left(\frac{y}{2\sqrt{t}}+\sqrt{Lt}\right)\right]$$
$$-\frac{yb}{4\sqrt{L}}\left[e^{-y\sqrt{L}}\operatorname{erfc}\left(\frac{y}{2\sqrt{t}}-\sqrt{Lt}\right)-e^{y\sqrt{L}}\operatorname{erfc}\left(\frac{y}{2\sqrt{t}}+\sqrt{Lt}\right)\right]$$
$$-\frac{\gamma bScSr}{\left(Sc-1\right)}\int_0^t\left[\frac{1}{\sqrt{\pi\left(t-s\right)}}+\gamma e^{\gamma^2(t-s)}\operatorname{erfc}\left(-\gamma\sqrt{t-s}\right)\right]$$
$$\times\left[\left(\tfrac{s}{2}-\tfrac{y}{4\sqrt{L}}\right)e^{-y\sqrt{L}}\operatorname{erfc}\left(\tfrac{y}{2\sqrt{s}}-\sqrt{Ls}\right)+\left(\tfrac{s}{2}+\tfrac{y}{4\sqrt{L}}\right)e^{y\sqrt{L}}\operatorname{erfc}\left(\tfrac{y}{2\sqrt{s}}+\sqrt{Ls}\right)\right]ds. \tag{22}$$

2) When $\mathrm{Pr}_{\mathrm{eff}}\neq 1$ and $Sc=1$,

$$C(y,t)=\operatorname{erf} c\left(\frac{y}{2\sqrt{t}}\right)-\frac{\mathrm{Pr}_{\mathrm{eff}}\,Sr}{\left(\mathrm{Pr}_{\mathrm{eff}}-1\right)}\left[e^{\left(c^2t-yc\sqrt{\mathrm{Pr}_{\mathrm{eff}}}\right)}\operatorname{erfc}\left(\frac{y}{2}\sqrt{\frac{\mathrm{Pr}_{\mathrm{eff}}}{t}}-c\sqrt{t}\right)-\operatorname{erfc}\left(\frac{y}{2}\sqrt{\frac{\mathrm{Pr}_{\mathrm{eff}}}{t}}\right)\right]$$
$$+\frac{\mathrm{Pr}_{\mathrm{eff}}\,Sr}{\left(\mathrm{Pr}_{\mathrm{eff}}-1\right)}\left[e^{\left(c^2t-yc\right)}\operatorname{erfc}\left(\frac{y}{2\sqrt{t}}-c\sqrt{t}\right)-\operatorname{erfc}\left(\frac{y}{2\sqrt{t}}\right)\right], \tag{23}$$

Maejo Int. J. Sci. Technol. **2015**, *9*(02), 224-245

$$u(y,t)=\frac{1}{4}e^{-i\omega t}\left[e^{-y\sqrt{L-i\omega}}\operatorname{erfc}\left(\frac{y}{2\sqrt{t}}-\sqrt{(L-i\omega)t}\right)+e^{y\sqrt{L-i\omega}}\operatorname{erfc}\left(\frac{y}{2\sqrt{t}}+\sqrt{(L-i\omega)t}\right)\right]$$
$$+\frac{1}{4}e^{i\omega t}\left[e^{-y\sqrt{L+i\omega}}\operatorname{erfc}\left(\frac{y}{2\sqrt{t}}-\sqrt{(L+i\omega)t}\right)+e^{y\sqrt{L+i\omega}}\operatorname{erfc}\left(\frac{y}{2\sqrt{t}}+\sqrt{(L+i\omega)t}\right)\right]$$
$$-\frac{Gm}{L}\left[e^{-y\sqrt{L}}\operatorname{erfc}\left(\frac{y}{2\sqrt{t}}-\sqrt{Lt}\right)+e^{y\sqrt{L}}\operatorname{erfc}\left(\frac{y}{2\sqrt{t}}+\sqrt{Lt}\right)-\operatorname{erf}c\left(\frac{y}{2\sqrt{t}}\right)\right]$$
$$-\frac{Gr}{L}\left[e^{\left(c^2t-yc\right)}\operatorname{erfc}\left(\frac{y}{2\sqrt{t}}-c\sqrt{t}\right)-\operatorname{erfc}\left(\frac{y}{2\sqrt{t}}\right)\right]$$
$$-\frac{1}{c^3}\left(a+\frac{dh}{Sc}\right)\left[e^{\left(c^2t-yc\sqrt{\mathrm{Pr}_{\mathrm{eff}}}\right)}\operatorname{erfc}\left(\frac{y}{2}\sqrt{\frac{\mathrm{Pr}_{\mathrm{eff}}}{t}}-c\sqrt{t}\right)-\operatorname{erfc}\left(\frac{y}{2}\sqrt{\frac{\mathrm{Pr}_{\mathrm{eff}}}{t}}\right)\right]$$
$$+\frac{1}{c^2}\left(a+\frac{dh}{Sc}\right)\left[2\sqrt{\frac{t}{\pi}}e^{-\frac{y^2\mathrm{Pr}_{\mathrm{eff}}}{4t}}-y\sqrt{\mathrm{Pr}_{\mathrm{eff}}}\operatorname{erfc}\left(\frac{y}{2}\sqrt{\frac{\mathrm{Pr}_{\mathrm{eff}}}{t}}\right)\right]$$
$$+\frac{1}{c}\left(a+\frac{dh}{Sc}\right)\left[\left(\frac{y^2\,\mathrm{Pr}_{\mathrm{eff}}}{2}+t\right)\operatorname{erfc}\left(\frac{y}{2}\sqrt{\frac{\mathrm{Pr}_{\mathrm{eff}}}{t}}\right)-y\sqrt{\mathrm{Pr}_{\mathrm{eff}}}\sqrt{\frac{t}{\pi}}e^{-\frac{y^2\mathrm{Pr}_{\mathrm{eff}}}{4t}}\right]$$
$$+\frac{Gr}{2\pi L}\int_0^t\left[\frac{yc}{s^{3/2}\sqrt{(t-s)}}e^{-\left(Ls+\frac{y^2}{4s}\right)}\right]ds-\frac{Gr}{2\sqrt{\pi}L}\int_0^t\left[\frac{yc^2}{s^{3/2}}e^{-\left(Ls+\frac{y^2}{4s}\right)}\right]ds$$
$$+ac\left(1+\frac{h}{Sc}\right)\int_0^t\left[\frac{1}{\sqrt{\pi(t-s)}}+ce^{c^2(t-s)}\operatorname{erf}c\left(-c\sqrt{t-s}\right)\right]$$
$$\times\left[\left(\tfrac{s}{2}-\tfrac{y}{4\sqrt{L}}\right)e^{-y\sqrt{L}}\operatorname{erf}c\left(\tfrac{y}{2\sqrt{s}}-\sqrt{Ls}\right)+\left(\tfrac{s}{2}+\tfrac{y}{4\sqrt{L}}\right)e^{y\sqrt{L}}\operatorname{erf}c\left(\tfrac{y}{2\sqrt{s}}+\sqrt{Ls}\right)\right]ds. \tag{24}$$

3) When $\mathrm{Pr}_{\mathrm{eff}}=1$ and $Sc=1$,

$$C(y,t)=\operatorname{erfc}\left(\frac{y}{2\sqrt{t}}\right), \tag{25}$$

$$u(y,t)=\frac{1}{4}e^{-i\omega t}\left[e^{-y\sqrt{L-i\omega}}\operatorname{erfc}\left(\frac{y}{2\sqrt{t}}-\sqrt{(L-i\omega)t}\right)+e^{y\sqrt{L-i\omega}}\operatorname{erfc}\left(\frac{y}{2\sqrt{t}}+\sqrt{(L-i\omega)t}\right)\right]$$
$$+\frac{1}{4}e^{i\omega t}\left[e^{-y\sqrt{L+i\omega}}\operatorname{erfc}\left(\frac{y}{2\sqrt{t}}-\sqrt{(L+i\omega)t}\right)+e^{y\sqrt{L+i\omega}}\operatorname{erfc}\left(\frac{y}{2\sqrt{t}}+\sqrt{(L+i\omega)t}\right)\right]$$
$$-\frac{Gm}{2L}\left[e^{-y\sqrt{L}}\operatorname{erfc}\left(\frac{y}{2\sqrt{t}}-\sqrt{Lt}\right)+e^{y\sqrt{L}}\operatorname{erfc}\left(\frac{y}{2\sqrt{t}}+\sqrt{Lt}\right)-2\operatorname{erfc}\left(\frac{y}{2\sqrt{t}}\right)\right]$$
$$+\frac{Gr}{L}\left[e^{(\gamma^2t-y\gamma)}\operatorname{erfc}\left(\frac{y}{2\sqrt{t}}-\gamma\sqrt{t}\right)-\operatorname{erfc}\left(\frac{y}{2\sqrt{t}}\right)\right]$$
$$-\frac{Gr}{2\pi L}\int_0^t\left[\frac{y\gamma}{s^{3/2}\sqrt{(t-s)}}e^{-\left(Ls+\frac{y^2}{4s}\right)}\right]ds+\frac{Gr}{2\sqrt{\pi}L}\int_0^t\left[\frac{y\gamma^2}{s^{3/2}}e^{-\left(Ls+\frac{y^2}{4s}\right)}\right]ds. \tag{26}$$

The dimensionless expression for skin friction evaluated from equation (20) is given by

Maejo Int. J. Sci. Technol. **2015**, *9*(02), 224-245

$$\tau = \frac{\tau'}{\rho U_0^2} = -\frac{\partial u}{\partial y}\Big|_{y=0},$$

$$= \frac{1}{2}\sqrt{L - i\omega}\, e^{-i\omega t}\left[1 - \operatorname{erfc}\left(\sqrt{(L - i\omega)t}\right)\right] + \frac{1}{2}\sqrt{L + i\omega}\, e^{i\omega t}\left[1 - \operatorname{erfc}\left(\sqrt{(L + i\omega)t}\right)\right]$$

$$+\left(\frac{a - d\,h}{c}\right)\sqrt{\mathrm{Pr}_{\mathrm{eff}}}\left[1 + e^{c^2 t}\left(-2 + \operatorname{erfc}\left(c\sqrt{t}\right)\right)\right] + 2\left(a - d\,h\right)\sqrt{\mathrm{Pr}_{\mathrm{eff}}}\sqrt{\frac{t}{\pi}}$$

$$+\left(\frac{b\,h}{c}\right)\sqrt{Sc}\left[1 + e^{c^2 t}\left(-2 + \operatorname{erfc}\left(c\sqrt{t}\right)\right)\right] + 2b\left(a + h\right)\sqrt{Sc}\sqrt{\frac{t}{\pi}}$$

$$+bt\sqrt{L}\left[1 - \operatorname{erfc}\left(\sqrt{Lt}\right)\right] + \frac{b}{2L}\left[1 - \operatorname{erfc}\left(\sqrt{Lt}\right)\right] + \frac{1}{\sqrt{\pi t}}e^{-Lt}$$

$$-c\left(a - d\,h + b\,h\right)\int_0^t \left[\frac{1}{\sqrt{\pi\left(t - s\right)}} + c\,e^{c^2(t-s)}\operatorname{erfc}\left(-c\sqrt{t - s}\right)\right]$$

$$\times\left[\sqrt{\frac{s}{\pi}}e^{-Ls} + \frac{(1 + 2Ls)}{2\sqrt{L}}\operatorname{erf}\left(\sqrt{Ls}\right)\right] ds, \tag{27}$$

where τ' is the dimensional skin friction. The dimensionless expression of the Nusselt number is given by

$$\mathrm{Nu} = -\frac{\nu}{U_0(T' - T_\infty)}\frac{\partial T'}{\partial y'}\Big|_{y'=0} = \frac{1}{\theta\left(0,t\right)} + 1,$$

$$= c\sqrt{\mathrm{Pr}_{\mathrm{eff}}}\left(1 + \frac{1}{e^{c^2 t}[1 + \operatorname{erf}\left(c\sqrt{t}\right)] - 1}\right). \tag{28}$$

The dimensionless expression of the Sherwood number is given by

$$\mathrm{Sh} = -\frac{\partial C}{\partial y}\Big|_{y=0},$$

$$= \sqrt{\frac{Sc}{\pi t}} + h\left(\sqrt{\mathrm{Pr}_{\mathrm{eff}}} - \sqrt{Sc}\right)c\,e^{c^2 t}\left[-2 + \operatorname{erfc}\left(c\sqrt{t}\right)\right]. \tag{29}$$

LIMITING CASES

In the Absence of Thermal-Diffusion Effect

In the absence of thermal-diffusion effect, which numerically corresponds to $Sr = 0$, the equations (19) and (20) reduce to:

$$C(y,t) = \operatorname{erfc}\left(\frac{y}{2}\sqrt{\frac{Sc}{t}}\right), \tag{30}$$

Maejo Int. J. Sci. Technol. **2015**, *9*(02), 224-245

$$
\begin{aligned}
u(y,t) = {} & \frac{1}{4}e^{-i\omega t}\left[e^{-y\sqrt{L-i\omega}}\operatorname{erfc}\left(\frac{y}{2\sqrt{t}}-\sqrt{(L-i\omega)t}\right)+e^{y\sqrt{L-i\omega}}\operatorname{erfc}\left(\frac{y}{2\sqrt{t}}+\sqrt{(L-i\omega)t}\right)\right] \\
& +\frac{1}{4}e^{i\omega t}\left[e^{-y\sqrt{L+i\omega}}\operatorname{erfc}\left(\frac{y}{2\sqrt{t}}-\sqrt{(L+i\omega)t}\right)+e^{y\sqrt{L+i\omega}}\operatorname{erfc}\left(\frac{y}{2\sqrt{t}}+\sqrt{(L+i\omega)t}\right)\right] \\
& -\frac{a}{c^2}\left[e^{\left(c^2t-yc\sqrt{\mathrm{Pr}_{\mathrm{eff}}}\right)}\operatorname{erfc}\left(\frac{y}{2}\sqrt{\frac{\mathrm{Pr}_{\mathrm{eff}}}{t}}-c\sqrt{t}\right)-\operatorname{erfc}\left(\frac{y}{2}\sqrt{\frac{\mathrm{Pr}_{\mathrm{eff}}}{t}}\right)\right] \\
& +\frac{a}{c}\left[2\sqrt{\frac{t}{\pi}}e^{-\frac{y^2\mathrm{Pr}_{\mathrm{eff}}}{4t}}-y\sqrt{\mathrm{Pr}_{\mathrm{eff}}}\operatorname{erfc}\left(\frac{y}{2}\sqrt{\frac{\mathrm{Pr}_{\mathrm{eff}}}{t}})\right)\right] \\
& +a\left[\left(\frac{y^2\mathrm{Pr}_{\mathrm{eff}}}{2}+t\right)\operatorname{erfc}\left(\frac{y}{2}\sqrt{\frac{\mathrm{Pr}_{\mathrm{eff}}}{t}}\right)-y\sqrt{\mathrm{Pr}_{\mathrm{eff}}}\sqrt{\frac{t}{\pi}}e^{-\frac{y^2\mathrm{Pr}_{\mathrm{eff}}}{4t}}\right] \\
& -b\left[\left(\frac{y^2Sc}{2}+t\right)\operatorname{erfc}\left(\frac{y}{2}\sqrt{\frac{Sc}{t}}\right)-y\sqrt{Sc}\sqrt{\frac{t}{\pi}}e^{-\frac{y^2Sc}{4t}}\right] \\
& +\frac{bt}{2}\left[e^{-y\sqrt{L}}\operatorname{erfc}\left(\frac{y}{2\sqrt{t}}-\sqrt{Lt}\right)+e^{y\sqrt{L}}\operatorname{erfc}\left(\frac{y}{2\sqrt{t}}+\sqrt{Lt}\right)\right] \\
& -\frac{yb}{4\sqrt{L}}\left[e^{-y\sqrt{L}}\operatorname{erfc}\left(\frac{y}{2\sqrt{t}}-\sqrt{Lt}\right)-e^{y\sqrt{L}}\operatorname{erfc}\left(\frac{y}{2\sqrt{t}}+\sqrt{Lt}\right)\right] \\
& +ac\int_0^t\left[\frac{1}{\sqrt{\pi(t-s)}}+ce^{c^2(t-s)}\operatorname{erfc}\left(-c\sqrt{t-s}\right)\right] \\
& \times\left[\left(\tfrac{s}{2}-\tfrac{y}{4\sqrt{L}}\right)e^{-y\sqrt{L}}\operatorname{erfc}\left(\tfrac{y}{2\sqrt{s}}-\sqrt{Ls}\right)+\left(\tfrac{s}{2}+\tfrac{y}{4\sqrt{L}}\right)e^{y\sqrt{L}}\operatorname{erfc}\left(\tfrac{y}{2\sqrt{s}}+\sqrt{Ls}\right)\right]ds,
\end{aligned}
\tag{31}
$$

the known solutions of Hussanan et al. [33] (see equations (20) and (22)). In addition, if we take $L=\omega=0$ and $\gamma=1,$ the solutions for temperature (18) and velocity (31) reduce to that obtained by Narahari and Nayan [34] (see equations (14) and (15)).

In the Absence of Mass Diffusion

In the absence of mass diffusion the solution for velocity given in equation (20) reduces to:

$$
\begin{aligned}
u(y,t) = {} & \frac{1}{4}e^{-i\omega t}\left[e^{-y\sqrt{L-i\omega}}\operatorname{erfc}\left(\frac{y}{2\sqrt{t}}-\sqrt{(L-i\omega)t}\right)+e^{y\sqrt{L-i\omega}}\operatorname{erfc}\left(\frac{y}{2\sqrt{t}}+\sqrt{(L-i\omega)t}\right)\right] \\
& +\frac{1}{4}e^{i\omega t}\left[e^{-y\sqrt{L+i\omega}}\operatorname{erfc}\left(\frac{y}{2\sqrt{t}}-\sqrt{(L+i\omega)t}\right)+e^{y\sqrt{L+i\omega}}\operatorname{erfc}\left(\frac{y}{2\sqrt{t}}+\sqrt{(L+i\omega)t}\right)\right] \\
& -\frac{a}{c^2}\left[e^{\left(c^2t-yc\sqrt{\mathrm{Pr}_{\mathrm{eff}}}\right)}\operatorname{erfc}\left(\frac{y}{2}\sqrt{\frac{\mathrm{Pr}_{\mathrm{eff}}}{t}}-c\sqrt{t}\right)-\operatorname{erfc}\left(\frac{y}{2}\sqrt{\frac{\mathrm{Pr}_{\mathrm{eff}}}{t}}\right)\right] \\
& +\frac{a}{c}\left[2\sqrt{\frac{t}{\pi}}e^{-\frac{y^2\mathrm{Pr}_{\mathrm{eff}}}{4t}}-y\sqrt{\mathrm{Pr}_{\mathrm{eff}}}\operatorname{erfc}\left(\frac{y}{2}\sqrt{\frac{\mathrm{Pr}_{\mathrm{eff}}}{t}})\right)\right]
\end{aligned}
$$

Maejo Int. J. Sci. Technol. **2015**, *9*(02), 224-245

$$+a\left[\left(\frac{y^2\,\mathrm{Pr}_{\mathrm{eff}}}{2}+t\right)\mathrm{erfc}\left(\frac{y}{2}\sqrt{\frac{\mathrm{Pr}_{\mathrm{eff}}}{t}}\right)-y\sqrt{\mathrm{Pr}_{\mathrm{eff}}}\sqrt{\frac{t}{\pi}}e^{-\frac{y^2\,\mathrm{Pr}_{\mathrm{eff}}}{4t}}\right]$$

$$+ac\int_0^t\left[\frac{1}{\sqrt{\pi(t-s)}}+ce^{c^2(t-s)}\mathrm{erfc}\left(-c\sqrt{t-s}\right)\right] \tag{32}$$

$$\times\left[\left(\tfrac{s}{2}-\tfrac{y}{4\sqrt{L}}\right)e^{-y\sqrt{L}}\mathrm{erfc}\left(\tfrac{y}{2\sqrt{s}}-\sqrt{Ls}\right)+\left(\tfrac{s}{2}+\tfrac{y}{4\sqrt{L}}\right)e^{y\sqrt{L}}\mathrm{erfc}\left(\tfrac{y}{2\sqrt{s}}+\sqrt{Ls}\right)\right]ds,$$

the known solution obtained by Hussanan et al. [35] (see equation (17)).

GRAPHICAL RESULTS AND DISCUSSION

We have solved the problem of unsteady MHD mixed convection flow in a porous medium past an oscillating vertical plate with constant mass diffusion and Newtonian heating in the presence of Soret and thermal radiation effects. Now it is very important to study the effects of all the parameters involved in the problem, i.e. Prandtl number (Pr), Grashof number (*Gr*), modified Grashof number (*Gm*), radiation parameter (*R*), magnetic parameter (*M*), porosity parameter (*K*), Schmidt number (*Sc*), Soret number (*Sr*), conjugate parameter (γ), time (t) and phase angle (ωt). Numerical results for velocity, temperature and concentration profiles are plotted in Figures 2-22, whereas skin friction, Nusselt number and Sherwood number are given in Tables 1-3.

The graph of the fluid velocity for different values of Pr are shown in Figure 2. From this Figure, it is observed that the velocity decreases with increasing values of Pr and velocity for electrolytic solution ($\mathrm{Pr}=1.0$) is greater than that for vapour ($\mathrm{Pr}=3.0$), water ($\mathrm{Pr}=7.0$) and engine oil (Pr = 100) in that order. Physically, a fluid with a large Prandtl number has high viscosity and small thermal conductivity, which makes the fluid thick and hence causes a decrease in velocity of the fluid. The effects of *Gr* and *Gm* on velocity profiles are examined in Figures 3 and 4. The velocity increases as *Gr* and *Gm* are increased, because an increase in both of these parameters means increasing thermal and mass buoyancy effects, which gives rise to an increase in the induced flow. Further, from these Figures, it is noticed that the Grashof number and modified Grashof number do not have any influence as the fluid moves away from the bounding surface.

The fluid velocity profiles are shown in Figure 5 for different values of R. It is found that the velocity increases with increasing values of R in the presence of thermal radiation (R = 2,3,4) as well as in the case of pure convection (R = 0). This is expected because higher radiation occurs when the temperature is higher and as a result the velocity increases. Effects of the magnetic parameter (*M*) on velocity are shown in Figure 6. Physically, $M=0$ means that there is no magnetic effect and the flow is purely hydrodynamic. It is found from this Figure that the velocity decreases with increasing value of M. This is expected as the application of the transverse magnetic field always results in a resistance-type force called Lorentz force. This force is similar in nature to a drag force, and upon increasing the values of M the drag force increases and tends to resist the fluid flow, thus reducing the fluid motion significantly. In order to visualise the velocity field in a porous medium, the profiles of velocity are illustrated in Figure 7 for different values of K, as the other flow parameters are kept fixed. It is observed that the velocity increases with an increase in K. This result may be explained by the fact that the presence of a porous medium decreases the resistance to flow and hence enhances the fluid motion. So it is confirmed from this graph that porosity has an important role in the present analysis.

Maejo Int. J. Sci. Technol. **2015**, *9*(02), 224-2

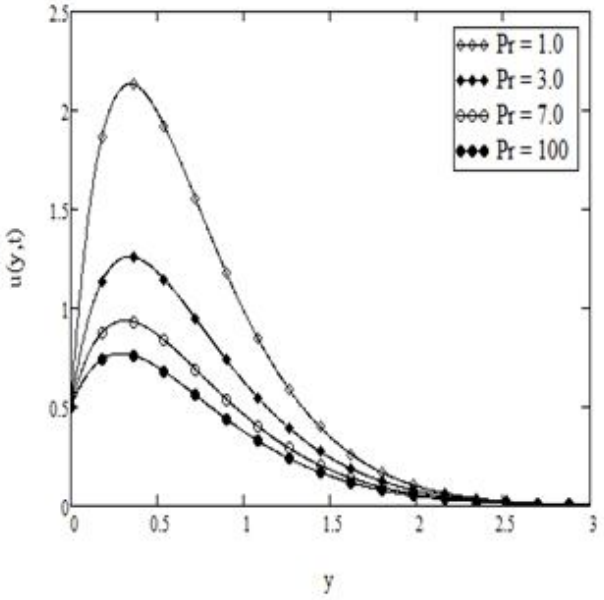

Figure 2. Velocity profiles for different values of Pr, when $Gr = 5, Gm = 2, R = 0.5, M = 2,$ $K = 0.5, Sc = 0.62, Sr = 2, \gamma = 1, t = 0.4, \omega t = \frac{\pi}{3}$

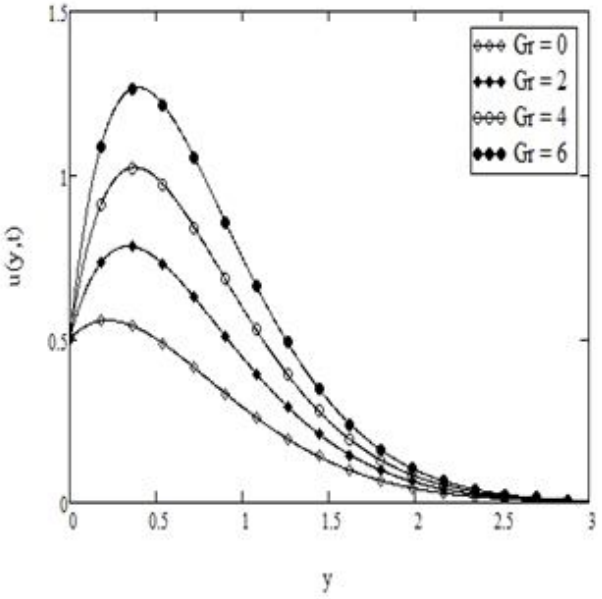

Figure 3. Velocity profiles for different values of Gr, when $\Pr = 1, Gm = 2, R = 0.5, M = 0.2,$ $K = 2, Sc = 0.62, Sr = 2, \gamma = 1, t = 0.4, \omega t = \frac{\pi}{3}$

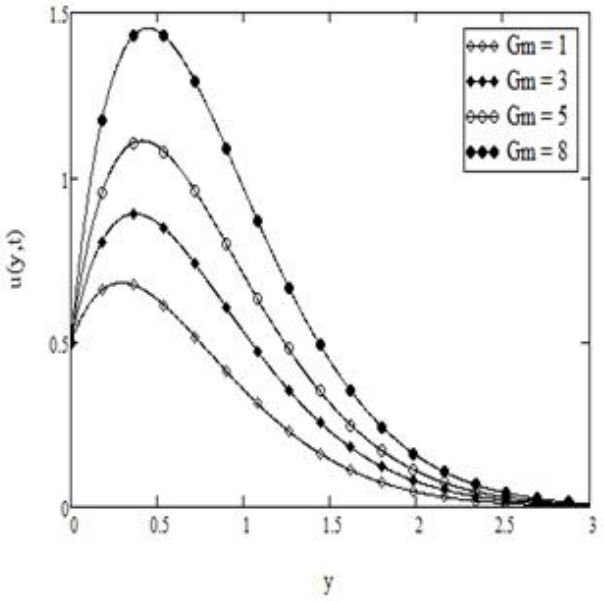

Figure 4. Velocity profiles for different values of Gm, when $\Pr = 1, Gr = 2, R = 0.5, M = 0.2,$ $K = 2, Sc = 0.62, Sr = 2, \gamma = 1, t = 0.4, \omega t = \frac{\pi}{3}$

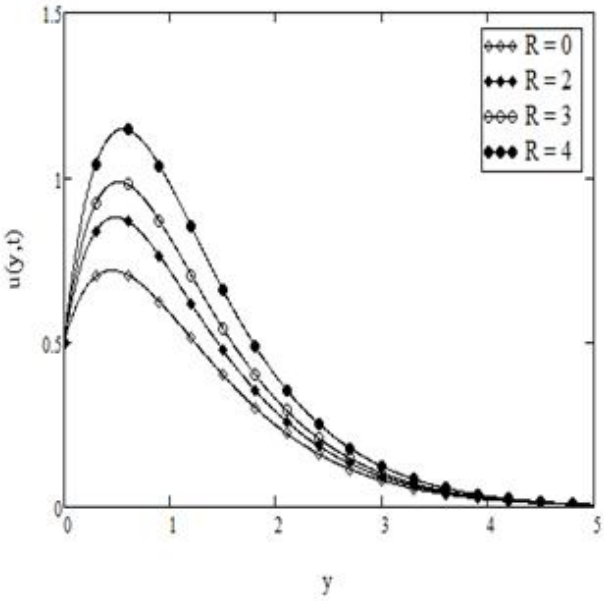

Figure 5. Velocity profiles for different values of R, when $\Pr = 7, Gr = 5, Gm = 2, M = 0.2,$ $K = 2, Sc = 0.22, Sr = 2, \gamma = 1, t = 0.5, \omega t = \frac{\pi}{3}$

Maejo Int. J. Sci. Technol. **2015**, *9*(02), 224-245

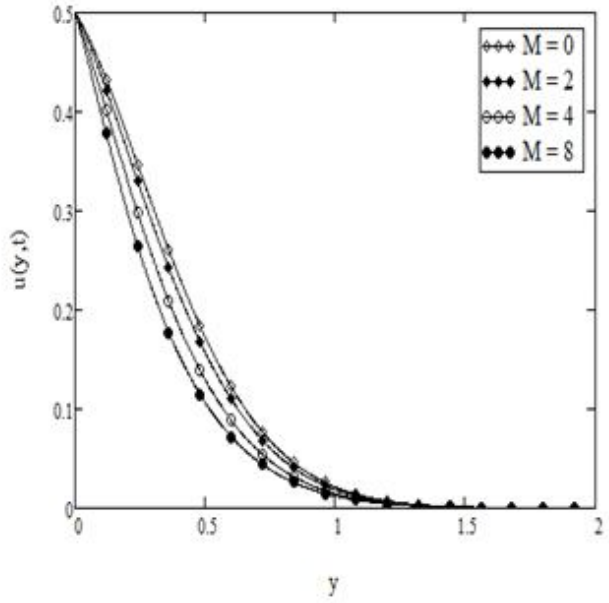

Figure 6. Velocity profiles for different values of M, when $\Pr = 3, Gr = 3, Gm = 2, Sc = 0.62,$ $R = 0.5, K = 0.5, Sr = 0.2, \gamma = 1, t = 0.1, \omega t = \frac{\pi}{3}$

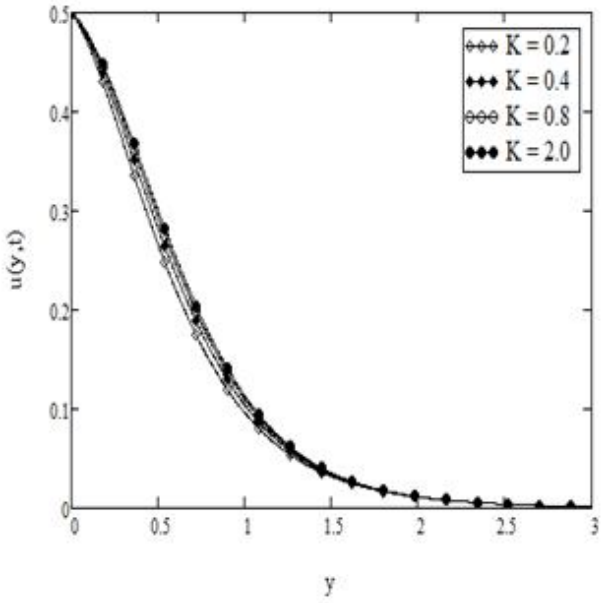

Figure 7. Velocity profiles for different values of K, when $\Pr = 1, Gr = 2, Gm = 1, Sc = 0.22,$ $R = 0.5, M = 0.2, Sr = 2, \gamma = 0.5, t = 0.2, \omega t = \frac{\pi}{3}$

The effects of Sc on the velocity profiles are shown in Figure 8. It is observed that an increase in Sc results in a decrease of velocity. Figure 9 shows that the fluid velocity increases with an increase in Sr. In Figure 10 the velocity profiles are illustrated for different values of γ; as the conjugate parameter increases, the fluid density decreases and the momentum-boundary-layer thickness increases, and finally the fluid velocity increases. From Figure 11, the fluid velocity increases with an increase in t. The velocity profiles for different values of ωt are shown in Figure 12. It is observed that the velocity shows an oscillatory behaviour: near the plate it is maximum and decreases with increasing distance from the plate, finally approaching zero as $y \to \infty$. It is clearly seen from this Figure that the velocity satisfies the given boundary conditions (13) and (14), which shows the accuracy of our results.

The effects of Prandtl number (Pr) on the fluid temperature are shown in Figure 13, which shows that the temperature decreases with an increase in Pr. Physically, this is due to the fact that with increasing Pr, the thermal conductivity of the fluid decreases and the viscosity of the fluid increases, and as a result the thermal boundary layer decreases. On the other hand, the buoyancy that results from the thermal expansion of the fluid adjacent to the surface causes the development of a rising boundary layer. Consequently, it is found from a comparison of Figure 2 and Figure 13 that the momentum boundary layer is thicker than the thermal boundary layer because the buoyant fluid layer causes macroscopic motion in the thicker fluid layer due to high viscosity.

The behaviour of the radiation parameter (R) on temperature profiles are shown in Figure 14, where $R = 0$ indicates no thermal radiation. It is observed that the temperature increases with an increase in R. This is due to the fact that the effect of thermal radiation is to increase the thermal-boundary-layer thickness with an increase in the value of the radiation parameter R. From Figure 15, it is found that as the conjugate parameter (γ) increases, so does the thickness of the thermal boundary layer and as a result the temperature of the plate increases. The effects of time (t) on the

Maejo Int. J. Sci. Technol. **2015**, *9*(02), 224-245

temperature (Figure 16) are quite identical to those on the velocity profiles, and it is observed from all the temperature profiles that the temperature is maximum near the plate and decreases away from the plate and finally approaches zero as $y \to \infty$.

The variations in the concentration field for different values of Pr and R are shown in Figures 17 and 18. An increase in Pr decreases the concentration field, but an increase in R increases the concentration field. Further, it is found from these Figures that the effects of Pr and R on the concentration field is similar to those on the velocity. Figure 19 illustrates the effects of Schmidt number (*Sc*) on the concentration field: an increase in the value of *Sc* makes the concentration boundary layer thick and hence the concentration field decreases. The effects of *Sr* on the concentration field are shown in Figure 20: the concentration increases with increasing value of *Sr*. From Figure 21, similar effects of the conjugate parameter (γ) on the concentration are found. The effects of time (t) on the concentration field (Figure 22) are similar to those on the velocity and temperature fields plotted in Figures 11 and 16 respectively.

The numerical values of skin friction, Nusselt number and Sherwood number for various parameters of interest are presented in Tables 1-3. The skin friction (τ) decreases with increasing t, R, Gm, Sc, Gr, K, γ and ωt, while it increases as Pr, Sr and M are increased (Table 1). The Nusselt number (Nu) increases with an increase in either Pr or γ, while the reverse effects are observed for t and R (Tabe 2). From Table 3, it is observed that the Sherwood number (Sh) increases with increasing value of Pr, Sc, Sr and γ, while it decreases with an increase in t and R.

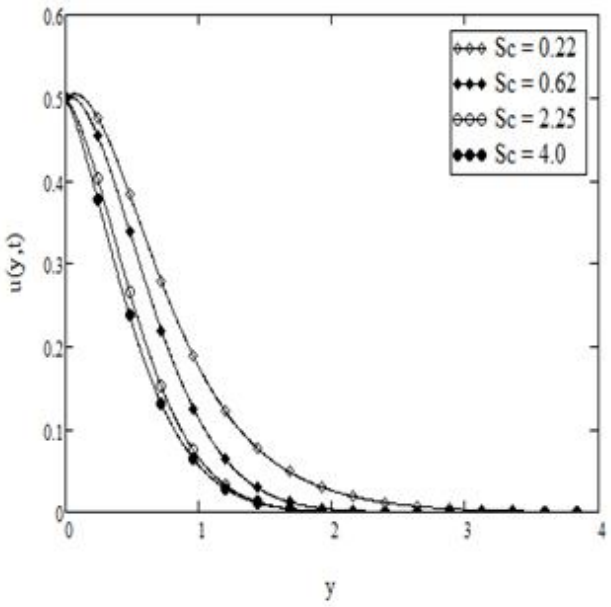

Figure 8. Velocity profiles for different values of Sc, when $\mathrm{Pr} = 3, Gr = 8, Gm = 2, R = 0.5, M = 0.2, K = 3, Sr = 2, \gamma = 0.2, t = 0.2, \omega t = \frac{\pi}{3}$

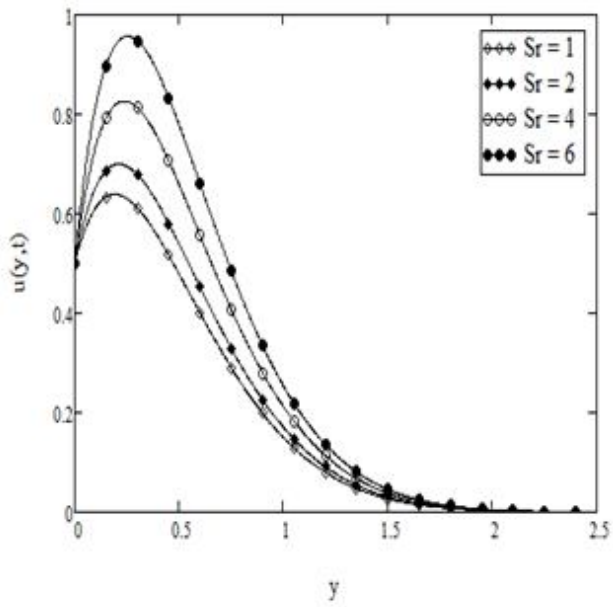

Figure 9. Velocity profiles for different values of Sr, when $\mathrm{Pr} = 3, Gr = 5, Gm = 3, Sc = 0.78, R = 0.5, M = 0.2, K = 0.5, \gamma = 1, t = 0.2, \omega t = \frac{\pi}{3}$

Maejo Int. J. Sci. Technol. **2015**, *9*(02), 224-245

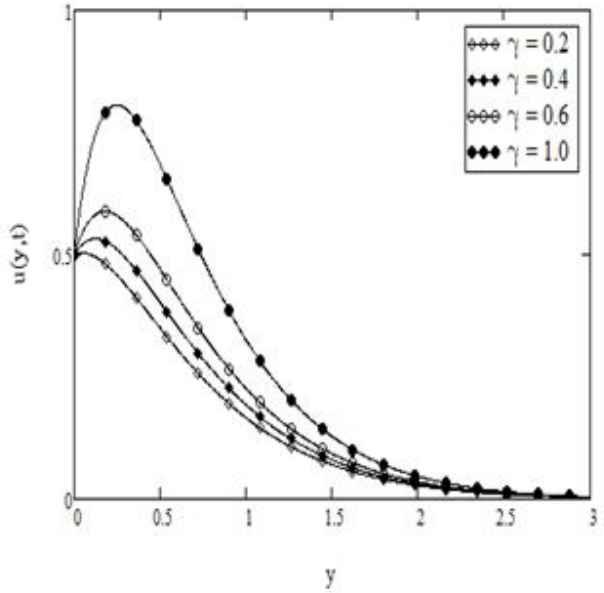

Figure 10. Velocity profiles for different values of γ, when $\Pr = 1, Gr = 5, Gm = 2, R = 3, M = 2,$ $K = 0.2, Sc = 0.22, Sr = 0.5, t = 0.2, \omega t = \frac{\pi}{2}$

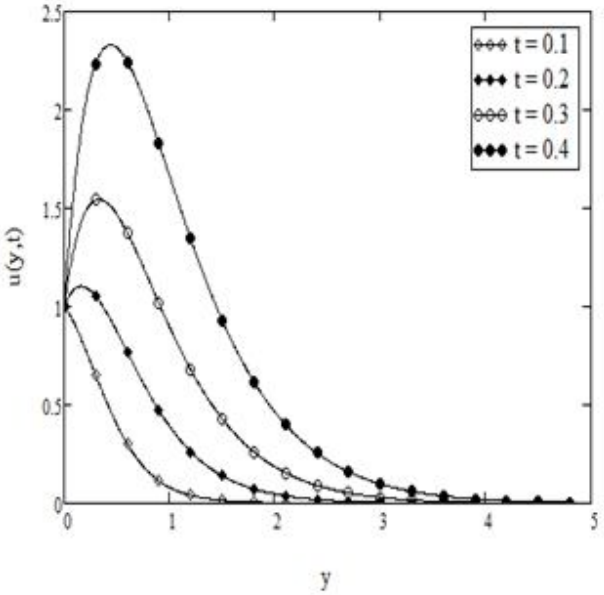

Figure 11. Velocity profiles for different values of t, when $\Pr = 1, Gr = 3, Gm = 2, R = 3, K = 2,$ $M = 0.2, Sc = 0.22, Sr = 0.5, \gamma = 1, \omega t = 0$

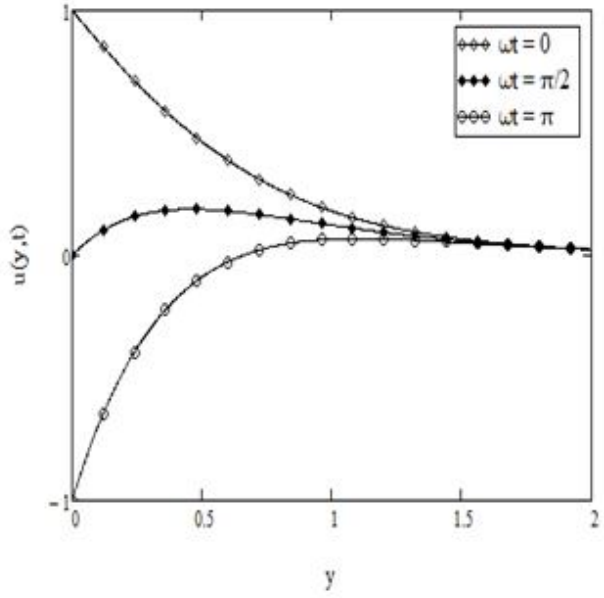

Figure 12. Velocity profiles for different values of ωt, when $\Pr = 7, Gr = 3, Gm = 2, R = 0.2,$ $M = 0.5, K = 0.2, Sc = 0.22, Sr = 2, \gamma = 0.1, t = 0.2$

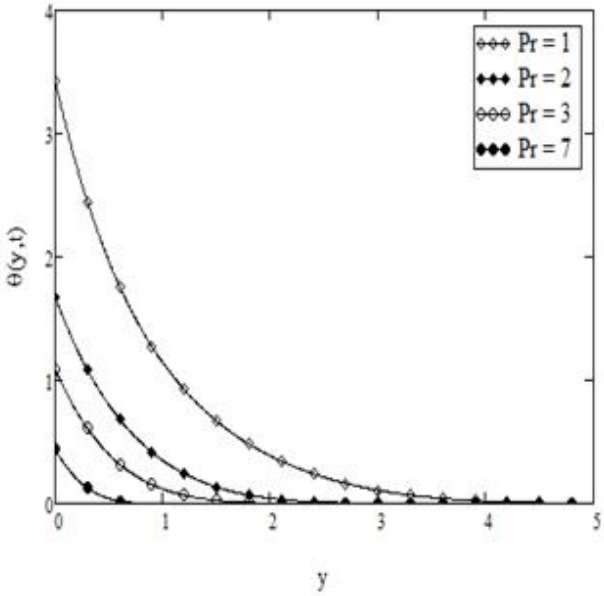

Figure 13. Temperature profiles for different values of Pr, when $t = 0.2, R = 3$ and $\gamma = 1$

Maejo Int. J. Sci. Technol. **2015**, *9*(02), 224-245

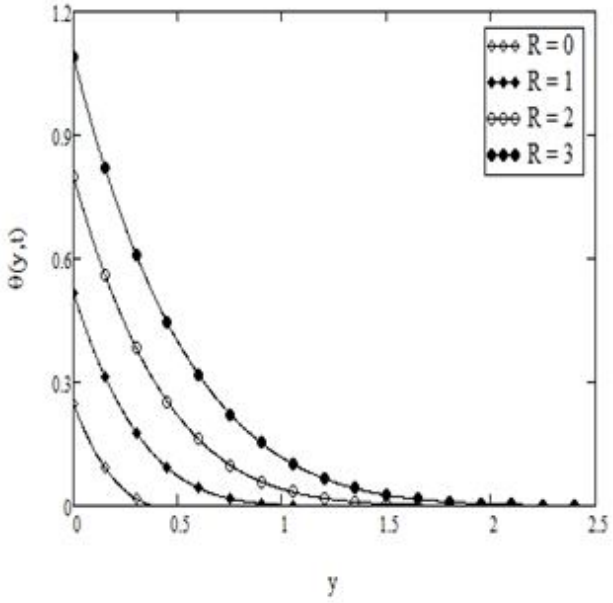

Figure 14. Temperature profiles for different values of R, when $t = 0.2, \mathrm{Pr} = 3$ and $\gamma = 1$

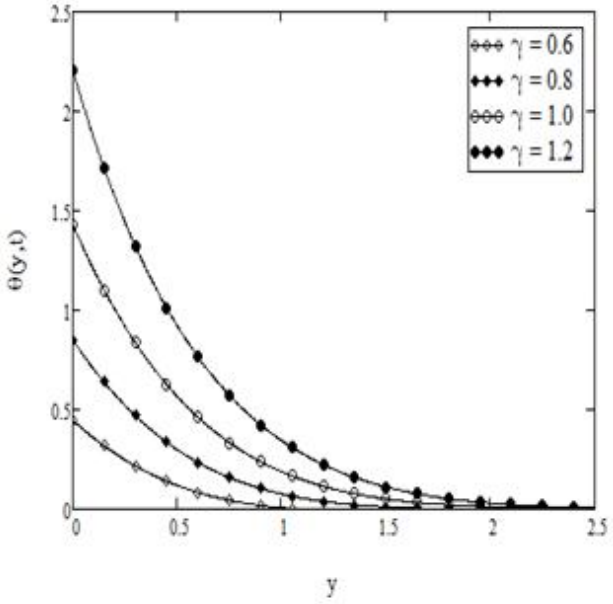

Figure 15. Temperature profiles for different values of γ, when $t = 0.4, \mathrm{Pr} = 3$ and $R = 2$

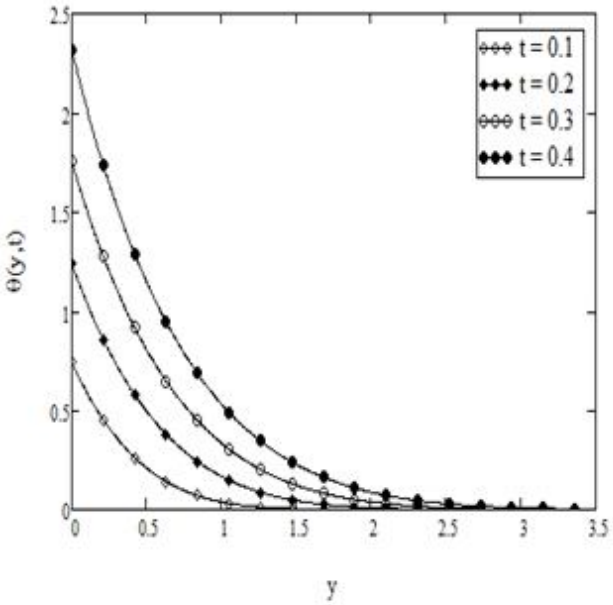

Figure 16. Temperature profiles for different values of t, when $R = 0.5, \mathrm{Pr} = 1$ and $\gamma = 1$

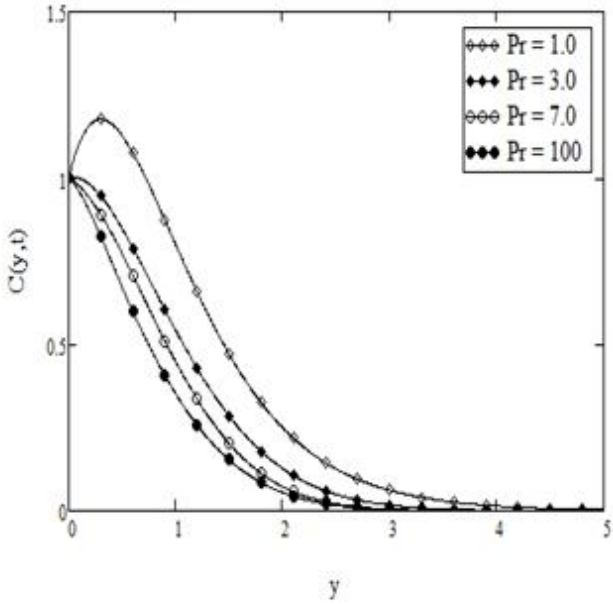

Figure 17. Concentration profiles for different values of Pr, when $t = 0.5, R = 3$, $\mathrm{Sc} = 0.94$, $\mathrm{Sr} = 0.5$ and $\gamma = 1$

Maejo Int. J. Sci. Technol. **2015**, *9*(02), 224-245

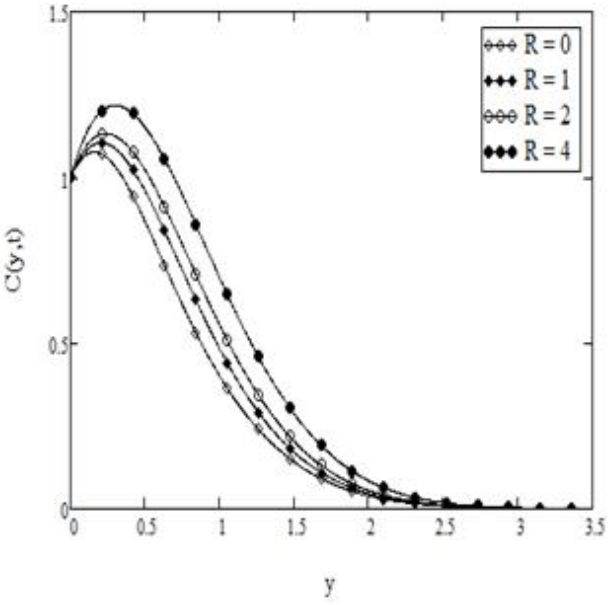

Figure 18. Concentration profiles for different values of R, when $t = 0.4, \Pr = 7$, $Sc = 0.94$, $Sr = 2$ and $\gamma = 1$

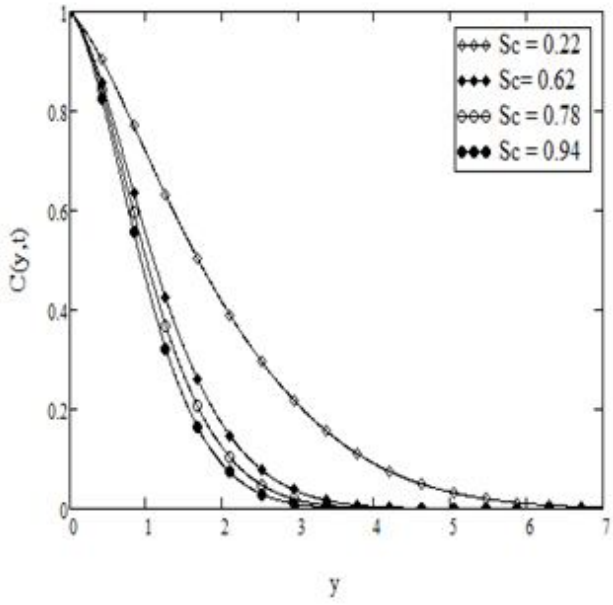

Figure 19. Concentration profiles for different values of Sc, when $t = 0.6, R = 0.8$, $\Pr = 7$, $Sr = 0.5$ and $\gamma = 1$

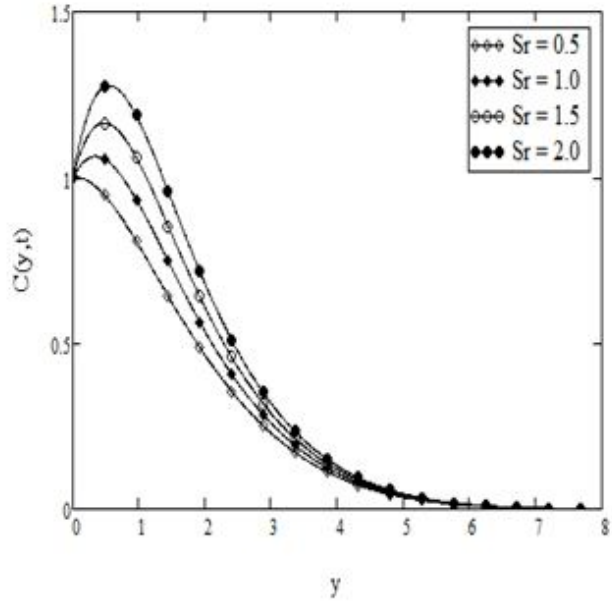

Figure 20. Concentration profiles for different values of Sr, when $t = 0.6, R = 3$, $\Pr = 7$, $Sc = 0.5$ and $\gamma = 1$

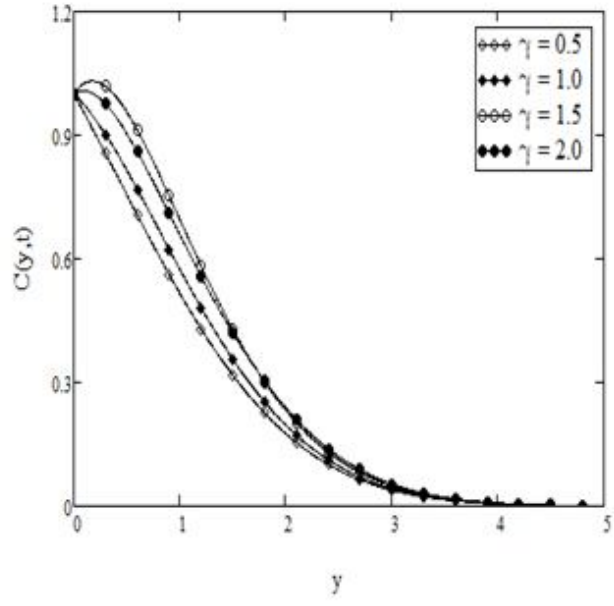

Figure 21. Concentration profiles for different values of γ, when $t = 0.8, R = 3$, $\Pr = 7$, $Sc = 0.78$ and $Sr = 0.2$

Maejo Int. J. Sci. Technol. **2015**, *9*(02), 224-245

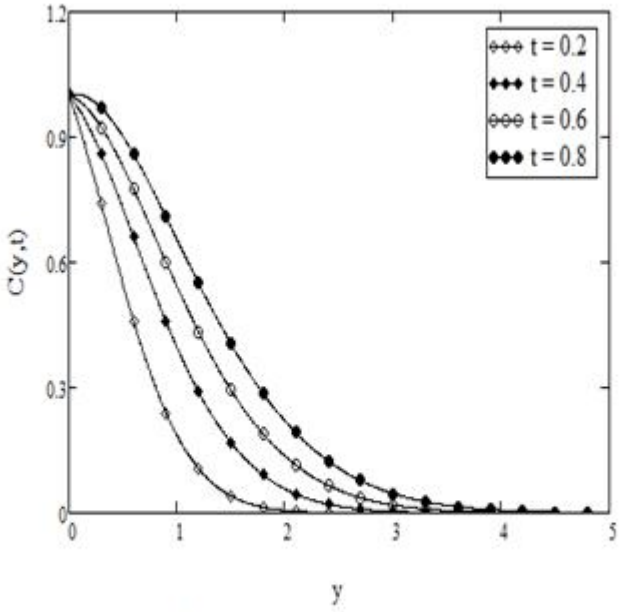

Figure 22. Concentration profiles for different values of t, when $R = 2, \Pr = 7$, $Sc = 0.78, Sr = 0.5$ and $\gamma = 1$

Table 1. Skin friction variations

t	R	Pr	Gr	Gm	Sc	Sr	M	K	γ	ω	τ
0.1	2	0.71	3	2	0.22	0.5	0.5	0.2	1.0	$\pi/2$	2.949
0.2	2	0.71	3	2	0.22	0.5	0.5	0.2	1.0	$\pi/2$	0.637
0.1	**4**	0.71	3	2	0.22	0.5	0.5	0.2	1.0	$\pi/2$	0.984
0.1	2	**1.0**	3	2	0.22	0.5	0.5	0.2	1.0	$\pi/2$	4.683
0.1	2	0.71	**4**	2	0.22	0.5	0.5	0.2	1.0	$\pi/2$	3.481
0.1	2	0.71	3	**3**	0.22	0.5	0.5	0.2	1.0	$\pi/2$	2.861
0.1	2	0.71	3	2	**0.62**	0.5	0.5	0.2	1.0	$\pi/2$	2.771
0.1	2	0.71	3	2	0.22	**1.0**	0.5	0.2	1.0	$\pi/2$	2.923
0.1	2	0.71	3	2	0.22	0.5	**1.0**	0.2	1.0	$\pi/2$	3.080
0.1	2	0.71	3	2	0.22	0.5	0.5	**0.4**	1.0	$\pi/2$	2.429
0.1	2	0.71	3	2	0.22	0.5	0.5	0.2	**1.5**	$\pi/2$	0.322
0.1	2	0.71	3	2	0.22	0.5	0.5	0.2	1.0	$\boldsymbol{\pi}$	2.757

Maejo Int. J. Sci. Technol. **2015**, *9*(02), 224-245

Table 2. Nusselt number variations

t	R	Pr	γ	Nu
0.2	2	0.71	1	1.3119
0.4	2	0.71	1	1.1054
0.2	**4**	0.71	1	1.1471
0.2	2	**1.0**	1	1.4659
0.2	2	0.71	**2**	2.0347

Table 3. Sherwood number variations

t	R	Pr	Sc	Sr	γ	Sh
0.2	2	0.71	0.22	0.5	1	0.5931
0.4	2	0.71	0.22	0.5	1	0.4205
0.2	**4**	0.71	0.22	0.5	1	0.5876
0.2	2	**1.0**	0.22	0.5	1	0.6024
0.2	2	0.71	**0.62**	0.5	1	0.9229
0.2	2	0.71	0.22	**1.0**	1	0.5946
0.2	2	0.71	0.22	0.5	**2**	0.5998

CONCLUSIONS

Exact solutions of magnetohydrodynamic mixed convection flow in a porous medium with Newtonian heating condition are obtained. Laplace transform technique is used for the problem solution. Graphs for temperature, concentration and velocity are plotted and discussed. The following main points concluded from this study are:

- Fluid velocity increases with increasing radiation parameter (R), Grashof number (Gr), modified Grashof number (Gm), porosity parameter (K) and conjugate parameter (γ).
- Skin friction behaviour is opposite to that of velocity.
- Nusselt number increases with increasing conjugate parameter and Prandtl number.
- Sherwood number increases with increasing Prandtl number, Schmidt number and conjugate parameter.

ACKNOWLEDGEMENTS

The authors gratefully acknowledge the financial support for this reasearch received from the Universiti Malaysia Pahang, Malaysia through vote numbers RDU140111 (FRGS) and RDU150101 (FRGS).

REFERENCES

1. R. A. Mohamed, S. M. A. Dahab and T. A. Nofal, "Thermal radiation and MHD effects on free convective flow of a polar fluid through a porous medium in the presence of internal heat generation and chemical reaction", *Math. Problems Eng.*, **2010**, *2010*, Art. ID 804719.
2. Seethamahalakshmi, G. V. R. Reddy and B. D. C. N. Prasad, "Unsteady MHD free convection flow and mass transfer near a moving vertical plate in the presence of thermal radiation", *Adv. Appl. Sci. Res.*, **2011**, *2*, 261-269.
3. P. Mebine and E. M. Adigio, "Effects of thermal radiation on transient MHD free convection flow over a vertical surface embedded in a porous medium with periodic boundary temperature", *Math. Aeterna*, **2011**, *1*, 245-261.
4. S. Suneetha, N. B. Reddy and V. R. Prasad, "Thermal radiation effects on MHD free convection flow past an impulsively started vertical plate with variable surface temperature and concentration", *J. Naval Archit. Marine Eng.*, **2008**, *2*, 57-70.

5. Z. Uddin and M. Kumar, "Radiation effect on unsteady MHD heat and mass transfer flow on a moving inclined porous heated plate in the presence of chemical reaction", *Int. J. Math. Model., Simulat. Appl.*, **2010**, *3*, 155-163.
6. R. Muthucumaraswamy and V. Valliammal, "MHD flow past an exponentially accelerated vertical plate with variable temperature and mass diffusion in the presence of chemical reaction", *Annals Fac. Eng. Hunedoara Int. J. Eng.*, **2012**, 151-154.
7. R. Nandkeolyar, M. Das and P. Sibanda, "Exact solutions of unsteady MHD free convection in a heat absorbing fluid flow past a flat plate with ramped wall temperature", *Bound. Value Probl.*, **2013**, *2013*, 247.
8. D. A. Nield and A. Bejan, "Convection in Porous Media", 2nd Edn., Springer, New York, **1999**.
9. D. B. Ingham, A. Bejan, E. Mamut and I. Pop (Eds.), "Emerging Technologies and Techniques in Porous Media", Springer, Dordrecht (Netherlands), **2004**.
10. O. A. Beg, J. Zueco, S. K. Ghosh and A. Heidari, "Unsteady MHD heat transfer in a semi-infinite porous medium with thermal radiation flux: Analytical and numerical study", *Adv. Numer. Anal.*, **2011**, *2011*, Art. ID 304124.
11. T. S. Reddy, M. C. Raju and S. V. K. Varma, "Unsteady MHD free convection oscillatory couette flow through a porous medium with periodic wall temperature in presence of chemical reaction and thermal radiation", *Int. J. Sci. Adv. Technol.*, **2011**, *1*, 51-58.
12. P. M. Kishore, V. Rajesh and S. V. Verma, "The effects of thermal radiation and viscous dissipation on MHD heat and mass diffusion flow past an oscillating vertical plate embedded in a porous medium with variable surface conditions", *J. Theoret. Appl. Mech.*, **2012**, *39*, 99-125.
13. F. Ali, I. Khan, Samiulhaq, N. Mustapha and S. Shafie, "Unsteady magnetohydrodynamic oscillatory flow of viscoelastic fluids in a porous channel with heat and mass transfer", *J. Phys. Soc. Jpn.*, **2012**, *81*, 064402-064402-8.
14. N. Ahmed and K. K. Das, "MHD mass transfer flow past a vertical porous plate embedded in a porous medium in a slip flow regime with thermal radiation and chemical reaction", *Open J. Fluid Dyn.*, **2013**, *3*, 230-239.
15. E. R. G. Eckert and R. M. Drake, Jr., "Analysis of Heat and Mass Transfer", McGraw Hill, New York, **1972**.
16. N. Ahmed, "Heat and mass transfer in Hartmann flow with Soret effect in presence of a constant heat source", *Turk. J. Phys.*, **2012**, *36*, 446-460.
17. M. Narayana, A. A. Khidir, P. Sibanda and P. V. S. N. Murthy, "Soret effect on the natural convection from a vertical plate in a thermally stratified porous medium saturated with non-Newtonian liquid", *J. Heat Transfer*, **2013**, *135*, 032501-032510.
18. F. Ali, I. Khan, S. Shafie and N. Musthapa, "Heat and mass transfer with free convection MHD flow past a vertical plate embedded in a porous medium", *Math. Probl. Eng.*, **2013**, *2013*, Art. ID 346281.
19. A. K. Jha, K. Choudhary and A. Sharma, "Influence of Soret effect on MHD mixed convection flow of visco-elastic fluid past a vertical surface with Hall effect", *Int. J. Appl. Mech. Eng.*, **2014**, *19*, 79-95.
20. B. K. Sharma, S. Gupta, V. V. Krishna and R. J. Bhargavi, "Soret and Dufour effects on an unsteady MHD mixed convective flow past an infinite vertical plate with Ohmic dissipation and heat source", *Afr. Matemat.*, **2014**, *25*, 799-821.

21. N. Vedavathi, K. Ramakrishna and K. J. Reddy, "Radiation and mass transfer effects on unsteady MHD convective flow past an infinite vertical plate with Dufour and Soret effects", *Ain Shams Eng. J.*, **2015**, *6*, 363-371.
22. R. K. Deka and S. K. Das, "Radiation effects on free convection flow near a vertical plate with ramped wall temperature", *Engineering*, **2011**, *3*, 1197-1206.
23. R. Muthukumaraswamy, "Natural convection on flow past an impulsively started vertical plate with variable surface heat flux", *Far East J. Appl. Math.*, **2004**, *14*, 99-119.
24. A. A. Dare and M. O. Petinrin, "Modelling of natural convection along isothermal plates and in channels using diffusion velocity method", *Maejo Int. J. Sci. Technol.*, **2010**, *4*, 43-52.
25. J. H. Merkin, "Natural-convection boundary-layer flow on a vertical surface with Newtonian heating", *Int. J. Heat Fluid Flow*, **1994**, *15*, 392-398.
26. D. Lesnic, D. B. Ingham, I. Pop and C. Storr, "Free convection boundary-layer flow above a nearly horizontal surface in a porous medium with Newtonian heating", *Heat Mass Transf.*, **2004**, *40*, 665-672.
27. M. Z. Salleh, R. Nazar and I. Pop, "Boundary layer flow and heat transfer over a stretching sheet with Newtonian heating", *J. Taiwan Inst. Chem. Eng.*, **2010**, *41*, 651-655.
28. M. Z. Salleh, R. Nazar, N. M. Arifin and I. Pop, "Forced-convection heat transfer over a circular cylinder with Newtonian heating", *J. Eng. Math.*, **2011**, *69*, 101-110.
29. S. Das, C. Mandal and R. N. Jana, "Radiation effects on unsteady free convection flow past a vertical plate with Newtonian heating", *Int. J. Comput. Appl.*, **2012**, *41*, 36-41.
30. A. R. M. Kasim, N. F. Mohammad, Aurangzaib and S. Sharidan, "Natural convection boundary layer flow of a viscoelastic fluid on solid sphere with Newtonian heating", *World Acad. Sci. Eng. Technol.*, **2012**, *64*, 628-633.
31. R. C. Chaudhary and P. Jain, "Unsteady free convection boundary-layer flow past an impulsively started vertical surface with Newtonian heating", *Roman. J. Phys.*, **2006**, *51*, 911-925.
32. P. Mebine and E. M. Adigio, "Unsteady free convection flow with thermal radiation past a vertical porous plate with Newtonian heating", *Turk. J. Phys.*, **2009**, *33*, 109-119.
33. A. Hussanan, Z. Ismail, I. Khan, A. G. Hussein and S. Shafie, "Unsteady boundary layer MHD free convection flow in a porous medium with constant mass diffusion and Newtonian heating", *Eur. Phys. J. Plus*, **2014**, *129*, 46. (doi 10.1140/epjp/i2014-14046-x)
34. M. Narahari and M. Y. Nayan, "Free convection flow past an impulsively started infinite vertical plate with Newtonian heating in the presence of thermal radiation and mass diffusion", *Turk. J. Eng. Environ. Sci.*, **2011**, *35*, 187-198.
35. H. Abid, M. A. Zakaria, Samiulhaq, I. Khan and S. Sharidan, "Radiation effect on unsteady magnetohydrodynamic free convection flow in a porous medium with Newtonian heating", *Int. J. Appl. Math. Stat.*, **2013**, *42*, 474-480.
36. M. Narahari and A. Ishak, "Radiation effects on free convection flow near a moving vertical plate with Newtonian heating", *J. Appl. Sci.*, **2011**, *11*, 1096-1104.
37. F. Ali, I. Khan, S. U. Haq and S. Shafie, "Influence of thermal radiation on unsteady free convection MHD flow of Brinkman type fluid in a porous medium with Newtonian heating", *Math. Probl. Eng.*, **2013**, *2013*, Art. ID 632394.
38. A. Hussanan, I. Khan and S. Shafie, "An exact analysis of heat and mass transfer past a vertical plate with Newtonian heating", *J. Appl. Math.*, **2013**, *2013*, Art. ID 434571.

Maejo Int. J. Sci. Technol. **2015**, *9*(02), 224-245

39. E. M. Sparrow and J. P. Abraham, "A new buoyancy model replacing the standard pseudo-density difference for internal natural convection in gases", *Int. J. Heat Mass Transf.*, **2003**, *46*, 3583-3591.
40. E. Magyari and A. Pantokratoras, "Note on the effect of thermal radiation in the linearized Rosseland approximation on the heat transfer characteristics of various boundary layer flows", *Int. Commun. Heat Mass Transf.*, **2011**, *38*, 554-556.